DYNAMICS OF PAVEMENT STRUCTURES

G. MARTINČEK

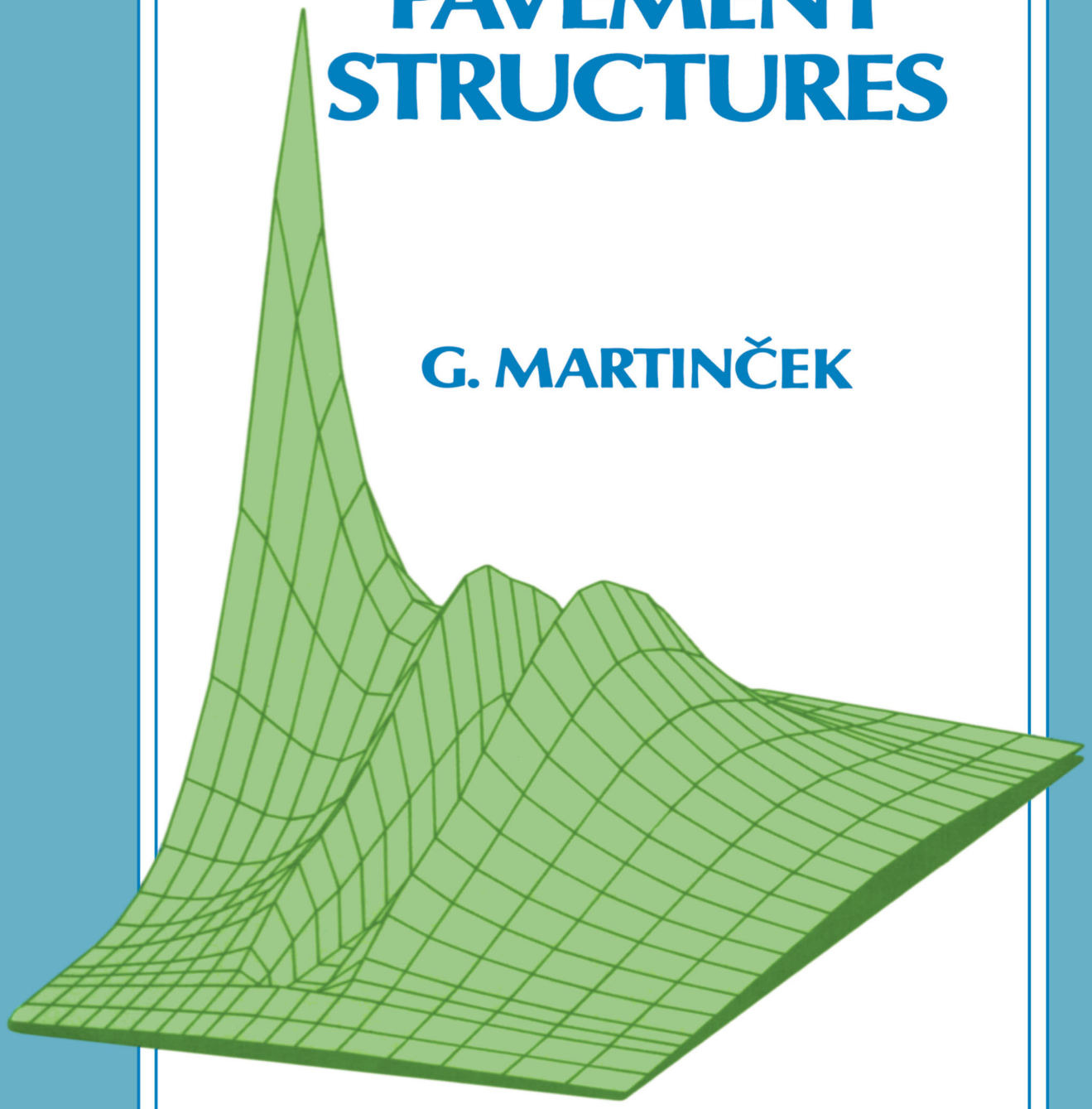

Taylor & Francis
Taylor & Francis Group

DYNAMICS OF PAVEMENT STRUCTURES

DYNAMICS OF PAVEMENT STRUCTURES

G. Martinček

Formerly Head of the Department of Dynamics
Institute of Construction and Architecture
Slovak Academy of Sciences
Bratislava, Slovak Republic

Taylor & Francis
Taylor & Francis Group
LONDON AND NEW YORK

By Taylor & Francis
2 Park Square, Milton Park, Abingdon, Oxon, OX14 4RN

Transferred to Digital Printing 2006

Co-published in with Ister Science Press Limited
Ister Science Press, Ltd., Staromestská 6, 811 03 Bratislava, Slovak Republic

ISBN (Taylor & Francis) 0 419 18100 8
ISBN (Ister Science Press) 80 88683 08 4

A catalogue record for this book is available from the British Library

Publisher's Note

The publisher has gone to great lengths to ensure the quality of this reprint but points out that some imperfections in the original may be apparent

CONTENTS

PREFACE

The basic criterion for the assessment of designs for pavement structures in highway and runway engineering, in terms of their service life and their operational characteristics, is their social effectiveness. Road surfaces must have the required bearing capacity and durability, and must provide for safe and comfortable driving over long periods. Specialists in transport engineering pay considerable attention to the improvement of material quality, reduction in the thickness of pavements, improvement in design methods and to other problems involved in the construction, operation and reconstruction of roads.

The loading of pavement structures is principally dynamic loading under mobile forces, the contact of which with the surface unevennesses of the pavement causes a dynamic state of stress. The current state of pavement design, in which these structures are designed only with regard to static loading, is basically a consequence of the insufficient development of dynamic theory, of the insufficient preparation of design engineers in dynamics, and of the absence of practical solutions. The aim of this book is at least partly to fill these voids, to inspire interest in the problem, and to strengthen the cooperation between specialists from industry and theoretical and research workers.

The starting point for developing the dynamics of pavement structures is detailed knowledge of the dynamic properties of materials and structures through the application and development of dynamic testing methods. This book summarizes data gathered over several years by the author and his team at the Institute of Civil Engineering and Architecture at the Slovak Academy of Sciences, in the developing field of dynamic investigation of road surfaces and road construction materials, based on the principle low-energy vibration methods.

Systematic experimental testing of real highway pavements carried out over several years and of various rigid and flexible pavement structures on the test track, served as the empirical basis for identifying acceptable theoretical models of pavement structures that agree closely with both the dynamic behaviour of structural materials and the

total dynamic reaction of road pavements and airfield runways. A layered pavement structure can be modelled in terms of an equivalent plate on a subgrade. The stress states determined by using the principle of this model were compared with the stresses determined by using the layered medium for a large number of various pavement structures, and they have shown substantial agreement. The fundamental advantage of the model of an equivalent plate on a subgrade is that it makes it possible to deal with the decisive and typical tasks of pavement dynamics, which cannot be solved in a simple way by using the model of the layered medium.

The aim throughout this book is to demonstrate practical application, and the differences between the dynamic and static approaches. It contains a considerable number of numerical examples in the sphere of pavement evaluation and design.

The importance of pavement dynamics is not just theoretical. As pavement dynamics develops, it should be able to give answers to the practical requirements of design engineers, and hence its importance will continually be increasing.

It is a pleasure to acknowledge the important contributions that Milan Pokorný and Jiří Špitálsky made during the preparation and development of the experimental arrangements and during the measurements of highway pavements.

Gustáv Martinček

LIST OF SYMBOLS

a	– radius of circular area
$a, \tilde{a}$	– acceleration
a_{ik}	– coefficients of equation system
a_k	– coefficients of Fourier series
a_{T}	– shift factor
$A_1, A_2, A_3, \ldots$	– anti-resonance extrema
A_{kj}	– coefficients of equation system
ARF	– amplitude reduction factor
b	– dimensionless parameter
b_{ik}	– coefficients of equation system
B, B_0, B_1, B_2	– barrier thicknesses
B_{kj}	– coefficients of equation system
B^*_ω	– complex bulk modulus
c, c_s	– phase velocities of stress-wave propagation
c_1	– velocity of dilatational waves
$c_2, c_{2\mathrm{I}}, c_{2\mathrm{II}}, c_{2\mathrm{s}}$	– velocities of shear waves
c_0, c_{01}	– velocities of longitudinal waves in one-dimensional medium
c_3	– velocity of longitudinal waves in two-dimensional medium
$c_{\mathrm{R}}, c_{\mathrm{Rz}}, c_{\mathrm{Rs}}$	– velocities of surface Rayleigh waves
c_{p}	– dimensionless speed of load
c_{kj}	– coefficients of equation system
C	– dimensionless phase velocity, measure of surface irregularities
C_{ba}	– barrier stiffness
$C_{\mathrm{p}}(\tau)$	– covariance
C_{P}	– dimensionless speed
d_{ik}	– coefficients of equation system
$D, \bar{D}, D^*$	– plate stifnesses, stiffness of layered system
D_1, D_2, D_k	– partial stiffnesses
D_{kj}	– coefficients of equation system

e – distance of central axis
E, E_ω, E_z, E_s – moduli of elasticity
E_{kj} – coefficients of equation system
E^*_ω, E^* – complex moduli of elasticity
E_1 – real part of complex modulus of elasticity
E_2 – imaginary part of complex modulus of elasticity
$f, f_l, f_t, f_{T_0}, f_T, f_a, f_b$ – frequencies
${}^F f$ – Fourier transform of function
F – dimensionless wave number, area
$\tilde{F}$ – harmonic variable force
F_{kj} – coefficients of equation system
$F_u, \widehat{F}_u$ – corner forces
$F(z)$ – auxiliary function
$F(i\omega)$ – frequency characteristic
g – gravitational acceleration
G, G_I, G_{II}, G_ω – shear moduli of elasticity
G^*_ω – complex shear modulus of elasticity
G_1, G_2, G_k – shear moduli of layer material
$G(r,t), G_0(r,t), G_{ba}$ – Green functions, fundamental solutions
G_{kj} – coefficients of equation system
h, h_i – plate or layer thickness
h_{eq} – thickness of equivalent plate or layer
$H_0^{(2)}, H_1^{(2)}$ – Hankel's functions
$H_n, \widehat{H}_n$ – equivalent shear forces
H_{kj} – coefficient of equation system
i – imaginary unit, integer
I – mass moment of inertia, parameter of global dynamic vehicle transfer
j – integer
J – moment of inertia
J_p – polar moment of inertia
J_t – modulus of stiffness in torsion
J_0, J_1 – Bessel's functions of the first kind
k – integer, real number
k_d – coefficient of mass increase
K_1 – coefficient of uniform compression
K_2 – coefficient of shear transmission
K_3 – coefficient of equivalent inertia
K^*_1, K^*_2 – complex stiffness characteristics

K_4^* – complex coefficient of nonlinear compression

$K_{ww}, K_{wp}, K_{wM},$
$K_{wQ}, \ldots K_{QQ}$ – influence functions

l – distance, length of cantilever element

l_0 – length of unevenness

L – distance, chosen length

m – mass

M – object mass, moment of torsion

$M, M_x, M_y,$
$M_{\mathrm{nn}}, \widehat{M}_{\mathrm{nn}}$ – bending moments

M_j – partial bending moment

$M_r, \widehat{M}_r$ – radial bending moments

$M_\varphi, M_{\mathrm{t}}, \widehat{M}_{\mathrm{t}}$ – tangential bending moments

${}^{\mathrm{F}}M, {}^{\mathrm{F}}M_2$ – Fourier transforms of bending moment

$M_{xy}, M_{\mathrm{nt}}, \widehat{M}_{\mathrm{nt}}$ – twisting moments

n – integer

N – number of nodal points

p, p_0 – intensity of normal load

${}^{\mathrm{H}}p$ – Hankel's load transform

${}^{\mathrm{F}}p$ – Fourier load transform

P – normal force

P_0 – force amplitude

P_1 – weight of unsprung load

P_2 – weight of spring-loaded part

$P_{\mathrm{k}}, P_{\mathrm{kk}}$ – right-hand sides of equation system

q – vertical reaction of half-space or subgrade

${}^{\mathrm{H}}q$ – Hankel's transform of subgrade reaction

$Q, Q_n, \widehat{Q}_n$ – shear forces, transverse forces

Q_j – partial shear force

$Q_{\mathrm{r}}, Q_{\mathrm{rs}}$ – transverse forces

${}^{\mathrm{F}}Q, {}^{\mathrm{F}}Q_0$ – Fourier transforms of transverse force

r – radial coordinate, radius of inertia

$\vec{r}$ – radius vector

R, R' – radius, variable distances

$R_1, R_2, R_3, \ldots$ – resonance extrema

${}^{\mathrm{F}}R$ – Fourier transform of dynamic load component

S – arbitrary component of state vector, region

S_0 – region

S_∞ – unbounded region

${}^{\mathrm{F}}S$ – Fourier transform of arbitraty state vector component

$S_p(\omega)$ – power spectral density
$S_s(\omega)$ – spectral density of state vector component
t – time coordinate
t_1 – dimensionless time
T – temperature, dimensionless time
T_0 – reference temperature
u_ϑ – tangential displacement
${}^H u$ – Hankel's transform of displacement
v – subgrade deflection, variable
V_s – coefficient of variation
w, w_0, w_1, w_2 – deflections, displacements
w_0 – depth of unevenness
w_L – linear deflection
${}^H w$ – Hankel's transform of displacement
${}^F w, {}^F w_0$ – Fourier transform of displacement
x – coordinate
y – coordinate
Y_0, Y_1 – Bessel's functions of the second kind
z – coordinate
z_0 – distance
Z^* – dimensionless mechanical impedance function
α, α_0 – wave number
α_1, α_2 – arguments
β – dimensionless frequency
γ – angular displacement, dimensionless characteristic of subgrade
γ_R, γ_J – real and imaginary part of angular displacement
γ_1, γ_2 – complex arguments
$\Gamma, \bar{\Gamma}$ – boundaries
$\delta, \delta_E, \delta_G, \delta_B$ – damping factors
$\delta(\xi), \delta(\eta_1)$ – Dirac generalized functions
Δ – curvature
$\Delta\varphi$ – phase difference
ε – strain, ratio of moduli
ε_0 – strain amplitude
$\varepsilon_{11}, \varepsilon_{12}, \varepsilon_{13}$ – ratios of velocities
ζ – dimensionless wave number
$\vec{\zeta}$ – radius vector of boundary point
η – argument, dimensionless coordinate, dimensionless wave number, ratio of wave lengths
η_1, η_2 – complex arguments

$\vec{\eta}$ – radius vector of boundary point
ϑ – logarithmic decrement, angle
$\vartheta, \vartheta_{\mathrm{w}}, \vartheta_{\mathrm{q}}, \vartheta_{\mathrm{M}}$ – dynamic coefficients
κ – function of Poisson's ratio, ratio of wave velocities
κ_0 – function of Poisson's ratio
$\Lambda, \Lambda_1, \Lambda_2, \Lambda_{\mathrm{i}}$ – wavelengths
μ, μ_{s} – Poisson's ratio
μ_0 – Poisson's ratio function
ν – speed of moving load
ξ – dimensionless coordinate
ξ_1, ξ_2 – arguments
$\vec{\xi}$ – radius vector of loading point
$\varrho, \varrho_{\mathrm{I}}, \varrho_{\mathrm{II}}, \varrho_{\mathrm{z}}, \varrho_{\mathrm{s}}$ – material densities
ϱ, ϱ' – variable distances
$\sigma, \sigma_x, \sigma_{\mathrm{r}}, \sigma_z, \sigma_{\mathrm{s}}$ – normal stresses
σ_0 – stress amplitude
${}^{\mathrm{H}}\sigma$ – Hankel's transform of stress
σ_{s}^2 – variance
$\tau, \tau_{xy}, \tau_{\mathrm{z}\vartheta}, \tau_{\mathrm{r}\vartheta}$ – tangential stresses
${}^{\mathrm{H}}\tau$ – Hankel's transform of stress
φ – phase angle, angle, angular displacement
${}^{\mathrm{F}}\varphi, {}^{\mathrm{F}}\varphi_0$ – Fourier transforms of angular displacement
φ_{kj} – angles between the radius vectors
$\varphi_1(\mu), \varphi_2(\mu)$ – functions of Poisson's ratio
ϕ, ϕ_1, ϕ_2 – functions of Poisson's ratio
ψ – ratio of densities
ω – angular frequency
Ω, Ω_0 – dimensionless frequencies
Ω_0 – parameter of pulse duration

INTRODUCTION

This book is an attempt to summarize and solve the problems connected with a very important but often neclected subject: the dynamics of pavement structures.

Chapter 1 deals with dynamic methods of diagnosis. The principle of the methods, the experimental technique, the measurement procedures and the basic theoretical assumptions make up the general framework of knowledge necessary for the practical application of the methods. Chapter 1 presents the mechanical impedance methods devised for use in testing viscous and elastic materials, and based on the principle of the forced vibration of the test bodies or the subgrade. From the point of view of practical applications, the main part of this chapter contains detailed and simplified procedures for measuring the phase velocities of the propagation of stress waves in flexible and rigid road surfaces, the interpretation of the measurement results, and methods for the determination of rigidity and elasticity characteristics of pavement sections. The methods described are complemented by numerous results obtained from measurement of real pavement structures under construction or already completed.

The model of an equivalent plate on subgrade, as the result of dynamic diagnosis, provides a dynamic theory that makes it possible to determine the dynamic deflection and the principal internal forces of real layered pavement structure. The relationships for the calculation of stresses in a layered pavement structure are presented in Chapter 2.

The various variants of the dynamic theory of an equivalent plate on subgrade are analysed in Chapter 3. From studies of the vibration of a layer in contact with half-space and stress-wave propagation in a layer on half-space without shear contact, attention is concentrated on the vibration of a plate on halfspace and on the technical theory of a plate on subgrade using a simplified dynamic model of the soil base. The solutions, in integral and closed form are complemented by numerous numerical results.

Chapter 4 presents studies performed in order to determine the state vector components under dynamic loading of a half-plate on subgrade,

of a plate strip on subgrade, of a plate on subgrade with joints and of a plate on inhomogeneous subgrade. All these problems have been solved by the reduction of a partial differential equation to an ordinary one using Fourier's integral transformation and by the application of the method of initial parameters. Numerous results of parametric numerical study have made it possible to compare the extreme values of flexural moments and subgrade reactions under particular schemes of dynamic loading for rigid and flexible pavements.

The typical problem of pavement dynamics is the dynamic interaction of the equivalent plate with the subgrade under a moving load. These problems are solved in Chapter 5 for a load moving along the boundary of a half-plate on subgrade. The solutions of the influence of periodical and isolated unevennesses under a moving load and load system with two degrees of freedom and the effect of a moving random load with extensive numerical data give well-arranged material for evaluating of the dynamic behaviour of rigid and flexible pavement structures.

Chapter 6 deals with the dynamic response of the equivalent plate with free boundaries on an unbounded soil base. Starting from derived fundamental solutions for the subgrade and a plate on subgrade, the boundary integral equations according to the theorem of reciprocity and their solution using boundary elements are presented with the numerical application on a square and rectangular plate on subgrade. The analysis of the dynamic response of a bounded plate resting on unbounded subgrade using the method of boundary elements confirms that the dynamic increment under a harmonic and pulse load is significant and that the derived procedures make it possible to obtain the corresponding dynamic coefficients.

The method of boundary integral equations offers us the possibility of studying very interesting problems concerning the influence of arbitrarily shaped holes in a plate on subgrade during the propagation of vibration. The results of the theoretical and numerical analysis are given in Chapter 7 and they confirm that the influence of the hole causes the concentration of vibration about the hole. The concentration is significant, especially at resonance frequencies, when the hole becomes an amplifier of vibration.

The dynamic response of an unbounded plate on a non-linear soil-base under stationary and pulsed loads is the subject of Chapter 8. Many numerical applications make it possible to evaluate the influence of non-linearity on the dynamic behaviour of an equivalent plate on subgrade.

The effects of vibration-isolating barriers in the soil base in the case

of vibration propagation evoked by traffic is analysed in Chapter 9. The application of the method of boundary elements for various kinds of barrier from different materials, trench barriers or sheet piling barriers offers advanced procedures for evaluating the vibration-isolating effect in the screening zone behind the barrier.

This book is probably the first attempt to summarize and solve systematically the main problems of pavement dynamics. It should be of interest not only to readers who are acquainted with the problems of pavement dynamics, but to students and skilled practising engineers as well.

1

DYNAMIC DIAGNOSIS OF PAVEMENT STRUCTURES

Dynamic diagnostic methods are based on the principle of the direct and indirect measurement of stress-wave velocities and their damping in the material medium.

Usually the vibration sources used have a small excitation energy. The testing is therefore non-destructive as the resulting dynamic stresses are slight and cannot affect the state of the original medium.

However, it is quite possible to use dynamic methods with a large excitation energy, which can be used to evaluate the bearing capacity of pavement structures and replace the static loading tests [1.1 – 1.3].

Dynamic testing can be classified according to the nature of the vibration process used into stationary vibration methods and pulse (impact) methods.

Stationary vibration methods use sources, that generate harmonic vibration at a specific frequency and inject it into the object under test. The applied frequency can be swept from the lowest frequencies to high ultrasonic frequencies.

The dynamic response of the object under test varies according to whether it is a bounded body, with dimensions comparable with the wavelength of the vibration process, or whether its dimensions are so large that it can be considered as an unbounded medium.

For a test sample that is a bounded body, a state of stationary forced vibration will arise characterized by amplitude and the phase of vibration motion at an arbitrary point of the sample. As the excitation frequency is changed, so the amplitude and phase angle of the resulting vibration will change and the phenomena of resonance and anti-resonance will result in extreme or significant values. Measurement of these extreme or significant amplitudes, together with the phase angles and corresponding frequencies, will provide parameters that can be used to assess the viscoelastic material characteristics of the test specimen.

If the harmonic exciting force is acting on an unbounded medium, such as a soil base or a structure with large dimensions like a pavement

structure, the process of stress-wave propagation will occur. The amplitude of the stress-waves diminishes with distance because of dispersion and damping. Measurement the stress-waves velocities and the corre-

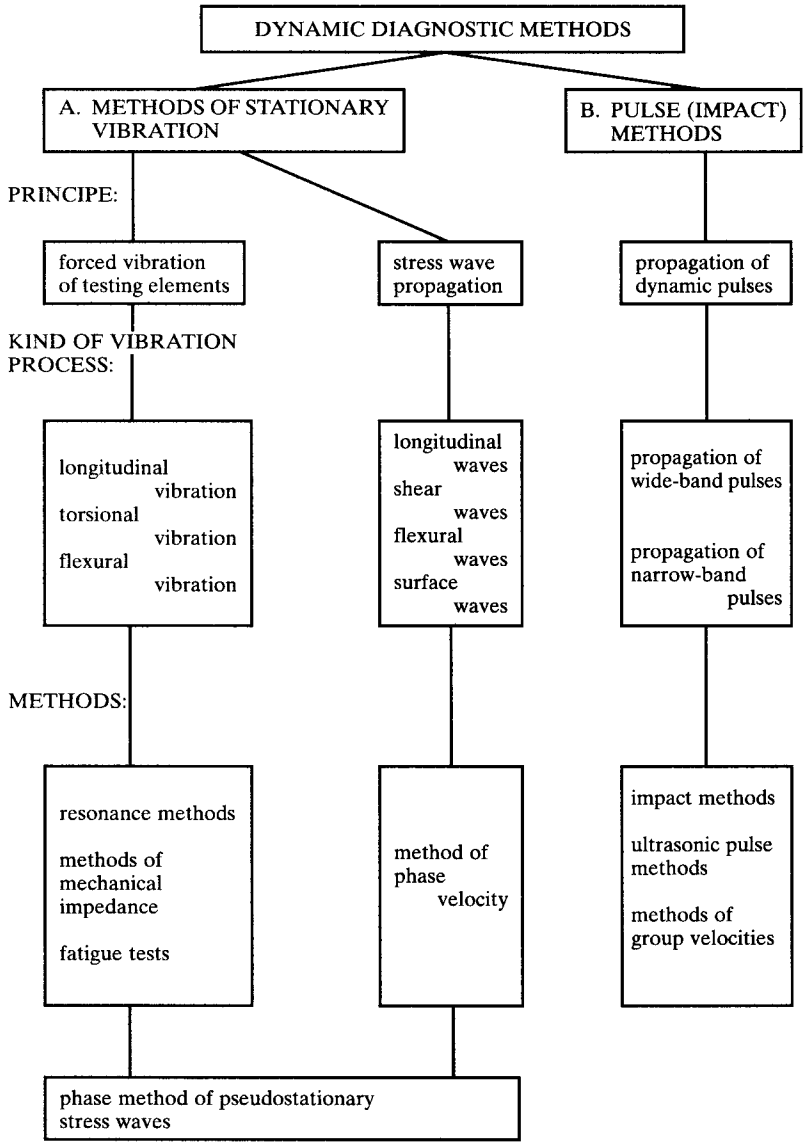

Fig. 1.1. Dynamic diagnostic methods.

sponding amplitudes of vibration provides parameters for assessing of the viscoelasticity and other characteristics of the tested structure.

The dynamic response of a medium or structure under pulse-impact force is the resultant effect of the spectrum of stress waves propagated in the medium. In practice the velocity of pulse propagation and the amplitude of vibration are used as parameters of the quality and properties of the tested structures or medium.

The various dynamic diagnostic methods are set out in Fig.1.1.

1.1 Stress-wave velocity measurement method

The method used to measure the velocity of the propagated stress waves is derived from the method of dynamic non-destructive testing, which is particularly advantageous for assessing the properties and characteristics of plane structures and elements.

The distinguished English specialist R. Jones in the sphere of non-destructive testing started to use stress-wave velocity measurement to assess the elasticity characteristics, and thickness of pavement structures over time and under the influence of traffic [1.4 – 1.6]. References [1.7 – 1.9] refer to the intensive investigation and search for possible applications of the stress-wave velocity method. The results of our investigations, in which the theoretical and methodical investigations are summarized, are given in references [1.10 – 1.15].

1.1.1 Principle of method and experimental technique

The method is based upon the principle of phase-velocity measurement, in which the phase difference is measured between the vibration of the source, which transmits sinusoidal stress waves of a set frequency into the test object, and the vibration of the pick-up. The pick-up is placed at various distances from the source, and a phase difference of 360° corresponds to change of a pick-up distance of about one wavelength.

The phase velocity of stress-wave propagation, c, is related to the frequency f by the relationship

$$c = f\Lambda. \tag{1.1}$$

The apparatus for measuring phase velocities is shown schematically in Fig. 1.2. The generator consists of (1) an electrodynamic or magnetostrictive vibrator, (2) a power amplifier, and (3) a sinewave generator whose frequency can be set at anything from 20 Hz to 25 kHz. The evaluation part consists of (4) an accelerometer, (5) a narrow-band filter and (6) a phasemeter that can measure from 0° to $360^\circ \pm 1^\circ$. The apparatus has a suitable power supply.

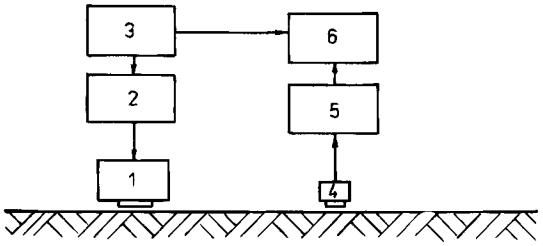

Fig. 1.2. Schematic diagram of apparatus for measuring phase velocities.

It can be seen from equation (1.1) that the decisive parameter is the wavelength Λ. Its determination can be realized in several ways.

First, if the wavelength Λ is small in comparison with the dimensions of the object, so that it is possible to take readings at a number of point, Λ is determined as follows.

1. The vibrator is acting at one point of the object.
2. The pick-up is moved along a selected line, and the phasemeter is used to determine the phase difference between the vibrator and the pick-up that corresponds to k times an angle of 360°.
3. The distance l that corresponds to the phase difference $k.2\pi$ is determined.
4. The wavelength Λ is given by the relationship $\Lambda = l/k$.

Second, if the wavelength is large and, because of the dimensions of the object or the power of the apparatus, measurements can only be made at a distance equalling one or a few wavelengths, then Λ is determined as follows.

1. The measuring line is set on the object and divided into an abscissa with equal intervals, such as 20, 10 or 5 cm.
2. The vibrator is placed at the starting point of the measuring line.
3. The pick-up location is changed to each of the discrete points of divided line in turn.

4. The phase difference is measured for every pick-up location.

5. The values of the phase angle are in a linear relationship with the pick-up distances and the slope of this linear relationship determines the average value of wavelength Λ.

Figure 1.3 shows a typical relationship between the measured phase angle φ and distance l. The results were obtained on the cement concrete plate of a pavement structure. The frequency of the vibration was $f = 28\,000$ Hz and the intervals of the points on the measuring line were 2.0 cm.

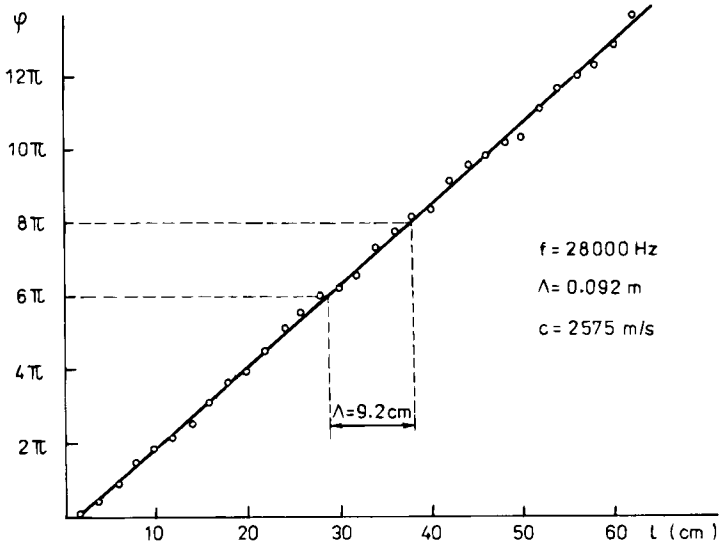

Fig. 1.3. Measured phase angle φ versus distance l.

Various disturbances can arise during the measurement process. The measurement precision is influenced by the nature of the pick-up's acoustic contact with the object at discrete points of the measuring line. This influence manifests itself as deviations in the linear relationship of φ versus l, as shown in Fig. 1.3.

Other reasons for disturbance exist in the bounded dimensions of the test object. The interference of direct and reflected waves, or the interference of waves of various kinds manifest themselves as a wave-like disturbance of the linear relationship of φ and l. This can be seen in Fig. 1.4 for a duralumin plate and longitudinal waves of frequency $f = 18\,000$ Hz.

The interference of direct and reflected waves in a bounded test object can give rise to standing waves at resonant frequencies. In such a rare case the measurement of wavelength is difficult.

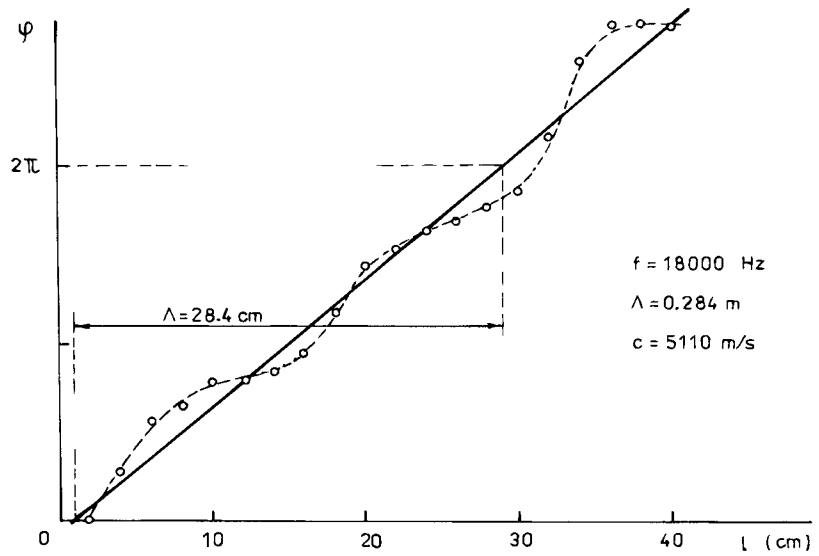

Fig. 1.4. Influence of reflected waves on relationship of phase angle to distance.

The third way in which the wavelength can be determined is by measuring the phase difference between the vibrations of two pick-up's the positions of which are constant [1.16]. This method makes it possible to automate measurement. The apparatus is shown schematically in Fig. 1.5. Two accelerometers (1, 2) with the same phase-frequency character-

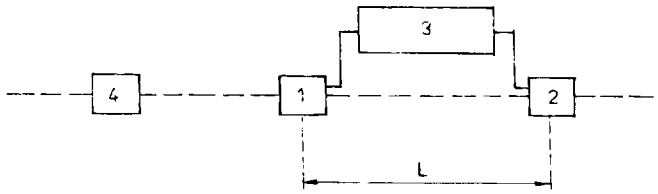

Fig. 1.5. Schematic diagram of apparatus for measuring phase difference.

istic are placed in contact with the tested object at a constant distance L. The outputs of the accelerometers are connected to the inputs of the phasemeter (3). The vibrator (4) transmits harmonic stress waves with frequency f into the tested medium. By the successive changing of frequency in the range $f_1 - f_n$ the phase difference $\Delta\varphi$ of accelerometer vibrations is measured. The distance L has to fulfil the condition $L < \Lambda_1$, if Λ_1 is the wavelength corresponding to the frequency f_1. By changing the frequency f, the phase difference $\Delta\varphi$ changes too. The phase difference $\Delta\varphi = 2\pi$ corresponds to the frequency when the wave-

length Λ is just equal to the distance L. The variation of $\Delta\varphi$ versus frequency f (Fig. 1.6) makes it possible to determine the wavelength Λ on the basis of the measured value $\Delta\varphi = k2\pi$ in the frequency range $(f_1, \ f_n)$. The wavelength is determined by the expression

$$\Lambda = \frac{2\pi L}{\Delta\varphi} = \frac{L}{k} \tag{1.2}$$

where k is an arbitrary real number.

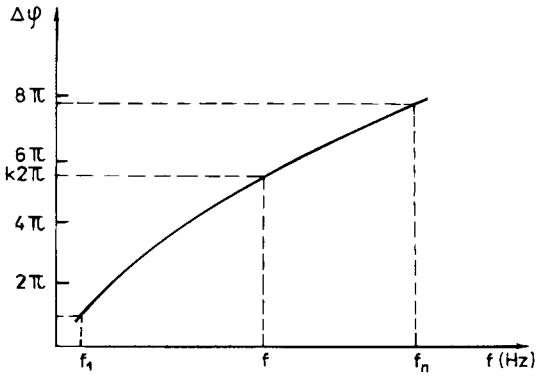

Fig. 1.6. Variation of phase difference $\Delta\varphi$ with frequency.

1.1.2 Theoretical assumptions

The theory underlying the problem of stress-wave propagation in a plane and layered medium is based on the assumption of a wider application of the phase velocity method.

Many questions of stress-wave propagation are known, especially in the geophysical literature, but the problems of layered pavement structures on a subgrade are theoretically so complex that they do not allow for exact numerical results to be obtained. This section can only outline the basics of the subject. For more detail, the reader is referred to special monographs, such as [1.17] and [1.18]. A study of the many problems of stress-wave propagation that are necessary for dynamic non-destructive diagnosis can be found in [1.13].

Dilatational and shear waves in unbounded media

It is well known that dilatational and shear waves propagate in a homogenous isotropic and elastic unbounded medium. They propagate with-

out dispersion: that is, their velocity does not depend on the frequency or the wavelength.

The velocity of dilatational waves, c_1, is determined by the relationship

$$c_1 = \left(\frac{E(1-\mu)}{\varrho(1+\mu)(1-2\mu)}\right)^{1/2} \tag{1.3}$$

in which E is the modulus of elasticity, ϱ is the density of the material and μ is Poisson's ratio.

The velocity of shear waves, c_2, is given by

$$c_2 = \left(\frac{G}{\varrho}\right)^{1/2} \tag{1.4}$$

if G is the shear modulus of elasticity.

The motion of mass particles in shear-wave propagation is perpendicular to the direction of wave propagation.

Surface stress waves on the half-space

The stress waves that propagate on the half-space surface and diminish with depth are termed, surface Rayleigh waves. In the isotropic, homogenous and elastic half-space they propagate without wave dispersion, and their velocity c_R is given by the frequency equation

$$\kappa^6 - 8\kappa^4 - (24 - 16\mu_0^2)\kappa^2 + (16\mu_0^2 - 16) = 0 \tag{1.5}$$

if

$$\kappa = \frac{c_R}{c_2} \tag{1.6}$$

and

$$\mu_0^2 = \frac{1-2\mu}{2(1-\mu)} \tag{1.7}$$

The velocity of surface-wave propagation, c_R, is always smaller than the velocity of shear waves, c_2. The values of the velocity ratios c_R/c_2 and c_R/c_0 in relationship to Poisson's ratio μ are given in Tab. 1.1. The

velocity c_0 of longitudinal waves in a one-dimensional medium is given by the very well-known relationship $c_0 = \sqrt{E/\varrho}$.

Table 1.1. Values of the velocity ratios.

μ	0	0.10	0.20	0.30	0.40	0.50
c_R/c_2	0.874	0.892	0.910	0.927	0.941	0.953
c_R/c_0	0.618	0.601	0.587	0.575	0.562	0.549

By using the method of phase velocities on pavement structures, the measured velocities at very high frequencies correspond to the velocity c_R of the surface layer medium, if the wavelength Λ is small compared with the surface layer thickness.

Symmetrical and asymmetrical stress waves in a plate with free surfaces

In an isotropic elastic plate (layer) with free surfaces, wave propagation is partly symmetrical, in view of the neutral plane of the plate (longitudinal waves), and partly asymmetrical (flexural waves).

The longitudinal stress waves are defined by the frequency equation

$$\frac{\tanh(sh/2)}{\tanh(qh/2)} = \frac{4\pi^2 h^2/\Lambda^2 (qh/2)(sh/2)}{\left[\pi^2 h^2/\Lambda^2 + (sh/2)^2\right]^2} \tag{1.8}$$

where

$$\frac{qh}{2} = \pi \frac{h}{\Lambda}\left(1 - \frac{c^2}{c_1^2}\right)^{1/2} \tag{1.9}$$

$$\frac{sh}{2} = \frac{\pi h}{\Lambda}\left(1 - \frac{c^2}{c_2^2}\right)^{1/2}. \tag{1.10}$$

The frequency equation (1.8) is fulfilled by a series of dispersion curves of phase velocity c. The velocity c of stress-wave propagation depends upon the ratio of plate thickness h to wavelength Λ. The variation of the first three branches of phase velocity versus the ratio h/Λ is shown in Fig. 1.7.

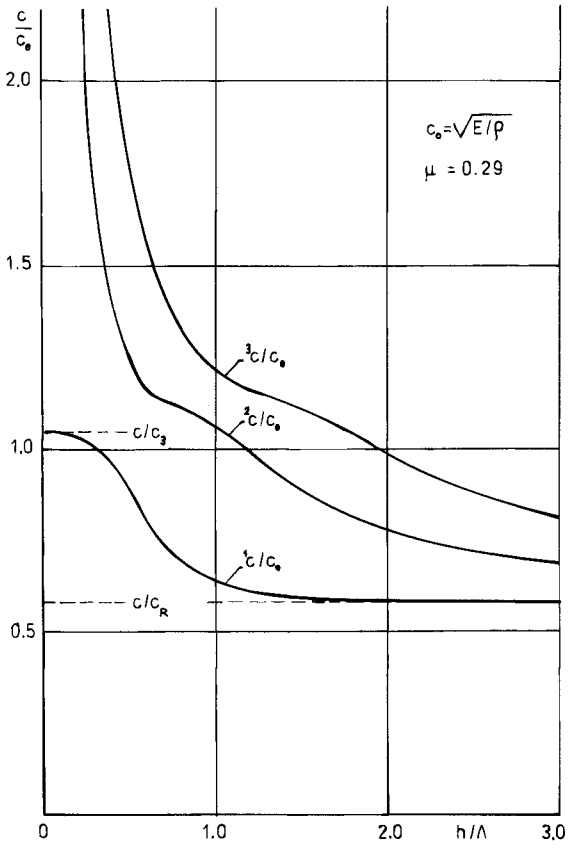

Fig. 1.7. Dispersion curves of phase velocity for symmetrical stress waves in a plate.

The first, fundamental branch of phase velocity begins from the value of velocity in the two-dimensional medium, c_3, by a large wavelength Λ according to the relationship

$$c_3 = \left(\frac{E}{\varrho(1-\mu^2)}\right)^{1/2}. \tag{1.11}$$

Succesively with the shortening of the wavelength the phase velocity c becomes smaller, and at very short values Λ is approaching the value of the surface-wave velocity, c_R.

The dispersion of flexural waves is determined by the frequency equation in the form

$$\frac{\tanh\,(qh/2)}{\tanh\,(sh/2)} = \frac{4\pi^2 h^2/\Lambda^2 (qh/2)(sh/2)}{\left[\pi^2 h^2/\Lambda^2 + (sh/2)^2\right]^2}. \tag{1.12}$$

The curves for the first three branches of phase velocity c are drawn in Fig. 1.8. The fundamental curve of the phase velocity starts at zero for $h/\Lambda \to 0$. The phase velocity increases with increasing h/Λ, and are approaching the value c_R at very short values of Λ or as $h/\Lambda \to \infty$.

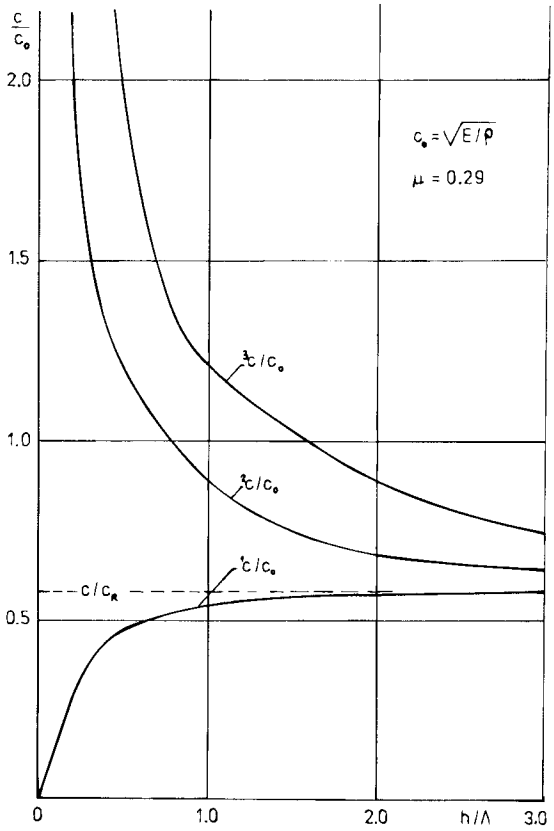

Fig. 1.8. Dispersion curves of phase velocity for asymmetrical stress waves in a plate.

The fundamental dispersion curve of the phase velocity for flexural waves in a plate is decisive for application to pavement structures.

Based on the results of detailed measurements of phase velocity in concrete and asphalt pavements it has been proved that the phase velocity corresponds to the characteristic course of this fundamental

dispersion curve. Naturally, the pavement structure is in contact with the subgrade and so the problem arises of how this contact influences the variation of the dispersion curve. Because of the difficult numerical solution of this problem, the influence of the subgrade was investigated experimentally on two-dimensional models and in a state of plane stress. The results of experiments on Duralumin models of various widths l in contact with an acrylic plane medium are plotted in Fig. 1.9. The variations of the dispersion curves of phase velocity for the first two branches of symmetrical waves (A_1, A_2) and the first two branches of asymmetrical waves (B_1, B_2) are identical to the theoretical courses for stress wave propagation in two-dimensional models with

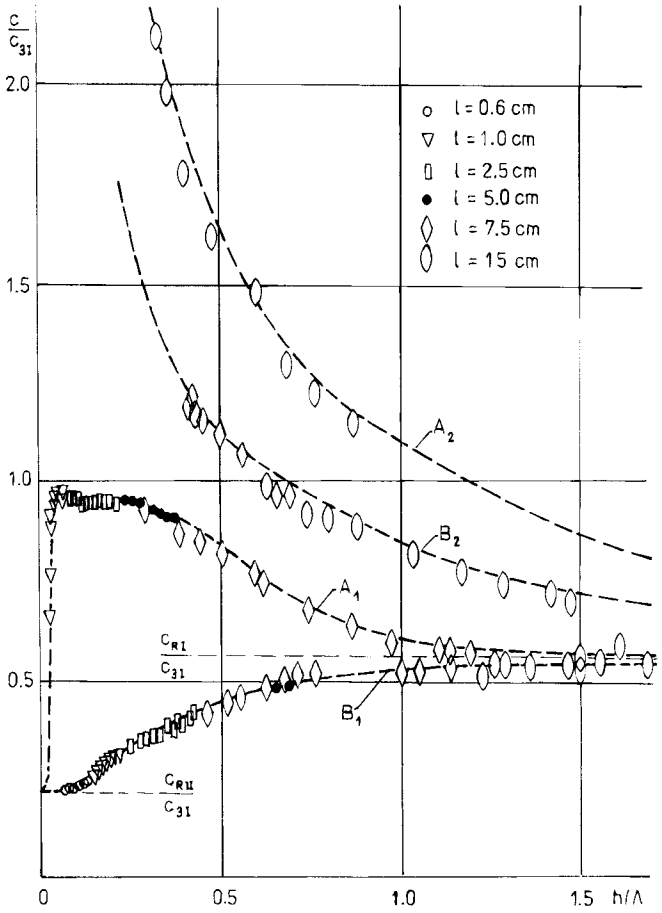

Fig. 1.9. Results of experiments on Duralumin models of various width l in contact with an acrylic plane medium.

free boundaries for the values $l/\Lambda > 0.10 - 0.15$ In the range of ratios $l/\Lambda < 0.10 - 0.15$ the courses of the experimental dispersion curves are different; the fundamental dispersion curves (A_1, B_1) are approaching the value of Rayleigh waves c_{RII} of the acrylic medium.

These results clearly prove that the fundamental dispersion curves for a plate with free surfaces may also be used for a plate on a subgrade for $h/\Lambda > 0.15$. At lower frequencies (that is at larger wavelength) the influence of the subgrade manifests itself in a marked change of the curves and the phase velocities approach the velocity of surface waves in the subgrade medium.

Because of the basic importance of the fundamental dispersion curve for flexural waves in a plate for the dynamic diagnosis of pavement structures, it is helpful to present the possibility of its calculation in an elementary way. We have established according to the theory of flexural vibration of the plate, considering the influence of shear and rotational inertia [1.14], relationships that give results identical to the values gained by the numerical solution of the transcendent equation (1.12).

The phase velocity c of the fundamental dispersion curve for flexural stress waves in the plate is given by the relationship

$$(c/c_0)^2 = p - \sqrt{p^2 - q} \tag{1.13}$$

where

$$p = \varphi_1(\mu) + \frac{\Lambda^2}{h^2}\varphi_2(\mu) \tag{1.14}$$

if

$$\varphi_1(\mu) = \frac{1}{2(1-\mu^2)} + \frac{\kappa_0}{4(1+\mu)} \tag{1.15}$$

$$\varphi_2(\mu) = \frac{3\kappa_0}{4\pi^2(1+\mu)} \tag{1.16}$$

$$\kappa_0 = \left(\frac{0.87 + 1.12\mu}{1+\mu}\right)^2 \tag{1.17}$$

and

$$q = \frac{\kappa_0}{2(1-\mu^2)(1+\mu)}$$

$$c_0 = \left(\frac{E}{\varrho}\right)^{1/2}. \tag{1.18}$$

Table 1.2 lists the values of the ratio c/c_0 as related to the ratios h/Λ and Poisson's ratio. The ratio $c/c_0 = 0$ for $h/\Lambda = 0$ and for $h/\Lambda \to \infty$ c/c_0 is given by

$$\frac{c}{c_0} = \left(\frac{\kappa_0}{2(1+\mu)}\right)^{1/2}. \tag{1.19}$$

Table 1.2. Values of the fundamental dispersion curve of flexural waves in the plate versus h/Λ and Poisson's ratio μ.

	h/Λ	0.1	0.2	0.3	0.4	0.6	0.8	1.0	1.5	2.0	3.0
	$\mu = 0$	0.197	0.314	0.390	0.455	0.511	0.548	0.565	0.590	0.598	0.603
	$\mu = 0.1$	0.192	0.313	0.389	0.448	0.509	0.541	0.560	0.580	0.592	0.596
$\frac{c}{c_0}$	$\mu = 0.2$	0.188	0.308	0.387	0.443	0.501	0.535	0.550	0.572	0.579	0.585
	$\mu = 0.3$	0.185	0.307	0.381	0.438	0.499	0.528	0.545	0.560	0.566	0.571
	$\mu = 0.4$	0.182	0.306	0.368	0.433	0.496	0.524	0.540	0.557	0.562	0.567
	$\mu = 0.5$	0.179	0.298	0.355	0.428	0.494	0.518	0.528	0.537	0.542	0.545

Shear stress waves in a layer on subgrade

Shear stress waves in a layer on subgrade with thickness h and with the polarization of the particles in motion in a horizontal plane are characterized by the frequency equation

$$G_{\mathrm{I}} d_{\mathrm{I}} \sin d_{\mathrm{I}} h - G_{\mathrm{II}} d_{\mathrm{II}} \cos d_{\mathrm{I}} h = 0 \tag{1.20}$$

where

$$d_{\mathrm{I}} = f_0 \left(\frac{c^2}{c_{2\mathrm{I}}^2} - 1\right)^{1/2} \tag{1.21}$$

$$d_{II} = f_0\left(1 - \frac{c^2}{c_{2II}^2}\right)^{1/2}. \tag{1.22}$$

G_I is the shear modulus of elasticity for the layer medium, G_{II} is the shear modulus of the subgrade material, f_0 is the wave number, and c_{2I}, c_{2II} are the velocities of shear waves in an unbounded medium of the layer or subgrade, given by

$$c_{2I} = \left(\frac{G_I}{\varrho_I}\right)^{1/2}, \qquad c_{2II} = \left(\frac{G_{II}}{\varrho_{II}}\right)^{1/2}. \tag{1.23}$$

A real solution of the frequency equation (1.20) exists if $c_{2I} < c_{2II}$, and in such a case Love's waves propagate at the surface of the system. The variations of the first three dispersion curves are plotted in Fig. 1.10 for $c_{2II}/c_{2I} = 2.437$. It can be seen that the phase velocities of stress-wave propagation are approaching to the velocity of shear waves in the layer, as h/Λ increases.

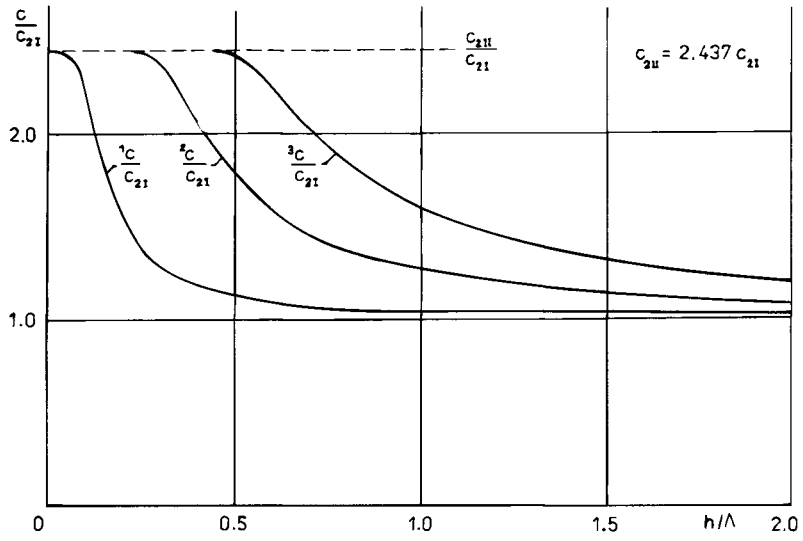

Fig. 1.10. Dispersion curves of Love's stress-wavevelocities in a layer on subgrade.

The other case is more important for pavement structures, when the plate or layer medium is stiffer than the subgrade medium. Then only a complex solution can be established, as the energy dispersion in the subgrade has to be included. The numerical solution of the frequency equation (1.20) indicates that the results are very similar to the results for the plate or layer with free surfaces. The contact with the subgrade manifests itself as energy dispersion in the subgrade, but the influence on the velocities is visible only at the lowest frequencies for the ratios $h/\Lambda < 0.1$, when the phase velocities are approaching the velocity of shear waves in the subgrade [1.19, 1.20].

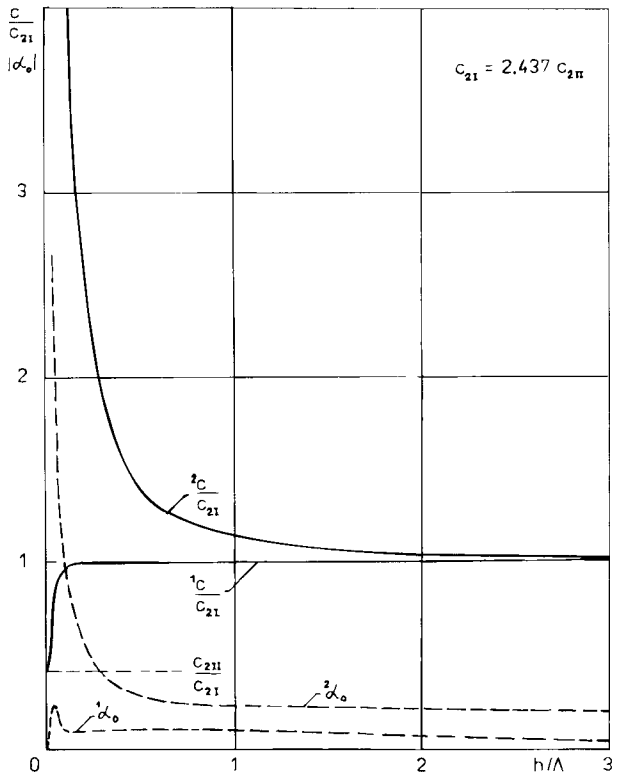

Fig. 1.11. Dispersion curves of shear stress waves in a layer on subgrade.

The first two dispersion curves for phase velocity c and dispersion coefficient α_0 are plotted in Fig. 1.11.

The problems of stress-wave propagation described above are only typical basic tasks, which can help in the understanding of wave disper-

sion and propagation in connection with the application of the method of phase velocities to pavement structures.

Of course, pavement structures are complicated multilayered systems on subgrade. The analysis of stress-wave propagation in such systems and numerical solutions are difficult. The other aspect of the behaviour of real pavement structures is the viscoelasticity of the material, especially in bitumen layers, cohesive soil layers and in the subgrade. These characteristics and the non-homogeneity of the materials, influence the results obtained by the assumption that the pavement layers and subgrade are elastic, isotropic and homogeneous media.

1.2 Mechanical impedance methods

The generally known resonance method belongs to the category of dynamic non-destructive methods. It presents a system of procedures for the determination of the modulus of elasticity of materials on the basis of measured natural frequencies of specimens or elements in various geometrical forms. Usually the fundamental natural frequencies are measured, which serve in the calculation of the elasticity characteristics using the corresponding theoretical relationships of vibration theory. It is possible to assess the logarithmic decrement of vibration as a damping characteristic after the width of the resonance curve.

These procedures can be applied without difficulty on concrete, ceramic and similar materials, but they fail when used for testing materials with distinct viscoelastic behaviour such as the bituminous materials of road construction or cohesive soil material. The considerable damping of such materials causes the resonance zone to weaken, and it may be suppressed to a such extent that the measurement cannot be realized.

The testing of viscoelastic materials on the principle of the forced vibration of specimens is possible by another way, using mechanical impedance methods .

1.2.1 Complex modulus of elasticity

The typical property of the viscoelastic behaviour of materials is the dependence of their elastic and damping characteristics on temperature

and loading time with respect to the frequency of the dynamic loading process.

The analysis of the dynamic response of structures made from viscoelastic materials, the theory of design and quality control require the assessment of their viscoelastic properties over a large range of temperatures and frequencies.

There are various formulations of viscoelastic behaviour in linear viscoelasticity, but the conception of complex modulus is the most useful [1.21 – 1.23]. Provided that the sinusoidal variable stress acts upon the element from the linear viscoelastic material, then the deformation of the element alters in time with the same frequency but a phase in arrears.

If the stress σ is expressed by the relationship

$$\sigma = \sigma_0 e^{i\omega t} \tag{1.24}$$

where σ_0 is the stress amplitude and ω is the angular frequency, then the strain ε is given in the form

$$\varepsilon = \varepsilon_0 e^{i(\omega t - \varphi)} \tag{1.25}$$

where φ is the phase angle.

The complex modulus of elasticity E^* established according to the relationships (1.24) and (1.25) is expressed by the equation

$$E^* = E_1 + iE_2 = \frac{\sigma}{\varepsilon} = \frac{\sigma_0}{\varepsilon_0} e^{i\varphi} \tag{1.26}$$

The real part of the complex modulus, E_1, is given by

$$E_1 = \frac{\sigma_0}{\varepsilon_0} \cos\varphi \tag{1.27}$$

and the imaginary part, E_2, is given by

$$E_2 = \frac{\sigma_0}{\varepsilon_0} \sin\varphi. \tag{1.28}$$

The absolute value of the complex modulus of elasticity is the ratio of stress and strain amplitudes expressed by the relationship

$$|E^*| = \frac{\sigma_0}{\varepsilon_0} = (E_1^2 + E_2^2)^{1/2}. \tag{1.29}$$

If the ratio of the imaginary and real parts of the complex modulus is indicated by the damping factor δ_E according to the relationship

$$\delta_E = \tan\varphi = \frac{E_2}{E_1} \tag{1.30}$$

the complex modulus of elasticity is given in the form

$$E^*_{\omega,T} = E_{\omega,T}(1 + i\delta_E) \tag{1.31}$$

and its absolute value is

$$|E^*_{\omega,T}| = E_{\omega,T}(1 + \delta_E^2)^{1/2}. \tag{1.32}$$

The subscripts ω and T refer to the value of complex modulus at a given frequency ω and temperature T. The coherence of the damping factor δ_E and the logarithmic decrement ϑ is determined by the approximate expression

$$\vartheta \approx \pi\delta_E. \tag{1.33}$$

The viscoelastic behaviour of a material for a given temperature is fully defined by the assessment of the values δ_E and $|E^*|$ for all frequencies.

The complex shear modulus or complex bulk modulus can be expressed in a similar way.

1.2.2 Function of mechanical impedance

The mechanical impedance at the driving point of the harmonic vibrating system is defined as the ratio of the exciting force to the velocity of motion at this point. It is the so-called mechanical impedance of the driving point and is a complex function.

If the motion velocity is related to another point, the complex ratio of the driving force and the motion velocity determines the so-called mechanical transfer impedance.

The inverse value of the mechanical impedance determines the mechanical mobility.

From the point of view of contemporary measurement techniques it is more advantageous to assess a normalized mechanical impedance Z^*, which is defined [1.22] as the ratio of the harmonic variable force $\tilde{F}$ to the product of acceleration $\tilde{a}$ at the driving point of the vibrating object and the object mass M

$$Z^* = \frac{\tilde{F}}{\tilde{a}M} \tag{1.34}$$

Z^* is a dimensionless complex function, the behaviour of which depends on the shape and dimensions of the vibrating object, and on the kind of vibration, and the elasticity and viscosity of the object material.

Mechanical impedance by flexural vibration

By using the flexural forced vibration of a tested object the most advantageous scheme in practice is the flexural vibration of a cantilever element at the free end of which a harmonic force $\tilde{F}$ is acting, or a test specimen with free ends and the exciting force $\tilde{F}$ in the middle of the specimen length. (Fig. 1.12).

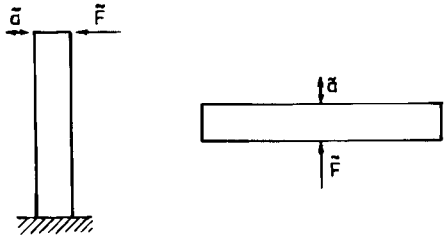

Fig. 1.12. Schematic diagram of mechanical impedance methods using flexural vibration of elements.

The cantilever testing element is satisfactory for bituminous pavement materials with appreciable damping. Normalized prismatic elements with dimensions $5 \times 5 \times 30$ cm or cylindrical elements may be used.

Many studies [1.24 – 1.29] have been performed in which the characteristics of the complex modulus of elasticity are determined after var-

ious schemes of element vibration, in which the amplitudes of force and deformation or deflection and the phase angle of the vibration process of these quantities are measured. All these procedures, theoretically often reduced in the system with one degree of freedom, have a common feature in that they can be applied only for very low frequencies below the fundamental natural frequency of the test element. Our effort is to prepare methods and procedures for the assessment of viscoelastic characteristics that would give the possibility of evaluating viscoelastic parameters in a wide frequency range by using just the resonance and anti-resonance frequencies of the tested element [1.30 – 1.35].

The normalized mechanical impedance for a cantilever element in flexural vibration without the influence of shear and rotational inertia is given by the relationship [1.14]

$$Z^* = \frac{1 + \cosh n^* l \cos n^* l}{n^* l(\cos n^* l \cosh n^* l - \sin n^* l \sinh n^* l)} \tag{1.35}$$

where

$$n^* l = \left(\frac{\omega^2 l^4 \varrho}{E_\omega^* r^2}\right)^{1/4} = \frac{nl}{(1 + \mathrm{i}\delta_E)^{1/4}} \tag{1.36}$$

if l is the length of the cantilever element, r is the radius of inertia of the cross section to the axis perpendicular to the vibration plane and

$$nl = \left(\frac{\omega^2 l^4 \varrho}{E_\omega r^2}\right)^{1/4}. \tag{1.37}$$

For use in practice it is preferable to establish the normalized mechanical impedance according Timoshenko's more accurate differential frequency of motion [1.36].

The variations of the calculated absolute value of normalized mechanical impedance in dB depending on the frequency parameter nl for the values of damping factor $\delta = 0.05$ and $\delta = 0.5$ are plotted in Fig. 1.13 The normalized mechanical impedance presents minima and maxima. The minima of the function $20 \log |Z^*|$, i.e. R_1, R_2, R_3,... represent resonances and correspond to the natural frequencies of an element that is clamped at the bottom and free at the top. The maxima A_1, A_2, A_3,... represent anti-resonances and correspond to the natural frequencies of